Available online at www.sciencedirect.com
SCIENCE DIRECT®
Journal of Nuclear Materials 337–339 (2005) 756–760
journal of nuclear materials
www.elsevier.com/locate/jnucmat

Radiation distribution and energy balance during type-I ELMs in ASDEX Upgrade

J.C. Fuchs *, T. Eich, A. Herrmann, K.F. Mast, The ASDEX Upgrade Team

MPI für Plasmaphysik, EURATOM Association, Boltzmannstr. 2, 85748 Garching, Germany

Abstract

Edge localised modes (ELMs) are a serious concern for plasma facing components in next generation tokamaks. Due to the limited capabilities of the commonly used bolometers reliable radiation data are generally only available with a time resolution of a few milliseconds, which is much larger than the power deposition time of type-I ELMs. Therefore an improved evaluation algorithm for bolometric data has been developed which allows to calculate the radiated energy on type-I ELM relevant timescales and to tomographically reconstruct the spatial distribution of the radiated energy during an ELM. This method has been used to investigate radiation during type-I ELMs in various plasma configurations. The spatial distribution of the radiated energy during an ELM shows that radiation losses are mainly located in the divertor. Up to 40% of the ELM energy loss are found as radiation. The energy balance is nearly fulfilled in most cases.

PACS: 52.55.Fa; 52.25.Vy; 52.40.Hf; 52.70.−m
Keywords: ASDEX Upgrade; ELM; Radiation; Power balance; Divertor plasma

1. Introduction

Edge localised modes (ELMs) are a serious concern for plasma facing components during H-mode discharges in next generation tokamaks. In ASDEX Upgrade about 50% of the ELM energy losses were found as target load in the divertor, and some 10–20% estimated on plasma facing components outside the divertor [1]. In order to understand the destinations of the ELM energy it is therefore necessary to estimate the radiated energy during an ELM. However, due to the limited capabilities of the commonly used thin foil metal resistor bolometer arrays in tokamaks and the usual data analysis, which includes a time derivation and therefore amplifies any noise in the measurements, reliable radiation data are generally only available with a time resolution of a few milliseconds, which is much larger than the power deposition time of type-I ELMs.

An improved evaluation algorithm for bolometric data has been developed and successfully implemented which allows to calculate the radiated energy on type-I ELM relevant timescales in ASDEX Upgrade. It is even possible to perform a tomographic reconstruction in order to obtain the spatial distribution of the radiated energy during an ELM in both the main plasma and especially the X-point and divertor region. This method

* Corresponding author. Tel.: +49 89 3299 1730; fax: +49 89 3299 2580.
E-mail address: christoph.fuchs@ipp.mpg.de (J.C. Fuchs).

0022-3115/$ - see front matter © 2004 Elsevier B.V. All rights reserved.
doi:10.1016/j.jnucmat.2004.09.054

has been used to investigate radiation during type-I ELMs in various plasma configurations.

In ASDEX Upgrade, radiation losses are measured with 100 bolometers placed in 7 pinhole cameras which are mounted in one poloidal cross section of the torus inside the vacuum vessel. Two bolometer pinhole cameras with 7 lines of sight each measure radiation from the inner and outer divertor leg and allow for a correction of the neutral gas pressure dependent bolometer sensitivity and of the residual bolometer offset drift. The region around the X-point is observed with an 8 channel pinhole camera, the main plasma with 72 bolometers placed in five cameras. The bolometers are miniaturised, low noise metal resistor bolometers [2] which are excited by a 50 kHz sine wave and effectively suppress thermal drift and electromagnetic interferences. They are non-blackened and sensitive over a spectral range from 0.1–200 nm.

2. Time resolution of bolometer data

Bolometers measure the change of the resistance of a metal foil due to the change of the foil temperature caused by the absorbed power. In tokamaks, this power mainly origins from radiation, but may also come from high energetic neutral particles generated in charge exchange processes. However, for ASDEX Upgrade, it has been shown with B2-Eirene simulations that the effect of these fast particles on bolometers is negligible compared to the absorbed radiation [3].

Usually, from the bolometer raw data (voltage at the bolometer bridge) the momentarily absorbed power is calculated by solving the bolometer equation

$$P(t) = C_{\mathrm{eff}}\left(\frac{\mathrm{d}\theta(t)}{\mathrm{d}t} + \frac{\theta(t)}{\tau_{\mathrm{eff}}}\right), \tag{1}$$

where $P(t)$ is the absorbed power, $\theta(t)$ is the measured voltage at the bolometer bridge, and C_{eff} and τ_{eff} are the effective heat capacity and time constant of the bolometer. However, Eq. (1) is valid only for time scales up to 1 kHz, since the approximations made for C_{eff} and τ_{eff} are no longer valid for higher frequencies and Eq. (1) must be replaced by a more complex equation involving device parameters and boundary conditions, which are normally not known [2].

The derivation $\mathrm{d}\theta/\mathrm{d}t$ in Eq. (1) is computed numerically, which implies that the usable time resolution is decreased. Furthermore, this derivation amplifies any noise in the raw data. Because of these two effects the radiated power calculated by Eq. (1) is normally not suited to get the radiated power during ELMs with a sufficient accuracy (trace (b) of Fig. 1).

However, we can calculate the accumulated energy $E(t)$ instead of the momentary power, by integrating Eq. (1)

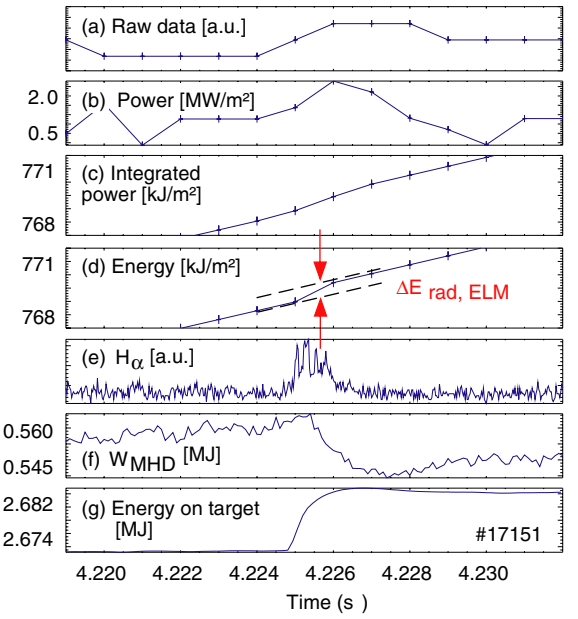

Fig. 1. Time traces of (a) bolometer raw data (voltage at bolometer bridge) corresponding to a line of sight looking through the inner divertor, (b) momentary power absorbed by this bolometer, calculated by Eq. (1), (c) accumulated energy (clipped) along this line of sight, calculated by integrating Eq. (1), (d) accumulated energy (clipped) along this line of sight, calculated by Eq. (2), where the increase of the radiated energy due to the ELM is indicated, (e) H_α radiation in the inner divertor, (f) plasma energy, and (g) heat load to the inner divertor target.

$$E(t) = C_{\mathrm{eff}}\left(\theta(t) + \frac{1}{\tau_{\mathrm{eff}}}\int \theta(t)\mathrm{d}t\right). \tag{2}$$

In this case we retain the time resolution of the raw data, and do not amplify the noise in the data.

During phases with constant absorbed power, the accumulated energy raises with a constant slope over several milliseconds, which can easily be determined. During an ELM however, there is a jump in the accumulated energy. The height of this jump corresponds to the radiated energy during the ELM along the line of sight of the particular bolometer (trace (d) of Fig. 1).

The height and time point of this jump corresponding to the radiated energy during an ELM is more accurately determined if the accumulated energy is calculated directly by Eq. (2) than by first calculating the power numerically with Eq. (1) and then again integrating it, since the derivation in Eq. (1) must be performed using several adjacent time points, such that the following integration gives only a smoothed trace of the accumulated energy. This effect can clearly be seen by comparing traces (c) and (d) from Fig. 1.

3. Radiation distribution during ELMs

Eq. (2) yields the radiated energy along the lines of sight of the particular bolometers. In order to obtain the spatial distribution of the radiated energy, one has to unfold these line integrals. This can be done with the 'anisotropic diffusion model tomography', which was originally developed for reconstructing the distribution of the radiated power [4], but is also applicable for the energy distribution. It takes into account that the variation of the radiation emissivity in the main plasma varies less along the magnetic field lines than perpendicular to them. This behaviour can be described mathematically by an anisotropic diffusion process with strongly different diffusion coefficients $D_\perp$ and $D_\parallel$ perpendicular and parallel to the magnetic field.

Fig. 2 shows the so obtained distribution of the radiated energy in a poloidal cross section of the divertor of ASDEX Upgrade during a time interval of 2 ms between ELMs and during an ELM for a discharge with 0.8 MA plasma current, 5 MW neutral beam injection power, density $\overline{n_e} = 5.8 \cdot 10^{19}\ \mathrm{m}^{-3} = 0.6 n_{GW}$, $q_{95} = 4.9$, and medium triangularity $\delta = 0.25$. Between ELMs (upper picture) we find radiation densities of up to 3.2 MW/m^3, nearly symmetrical distributed between the inner and outer divertor. The averaged radiated power is 2.7 MW, which is about 53% of the input power. During the ELM with a loss of plasma energy of 13.4 kJ (lower picture) we find radiation densities, which are twice as high than between ELMs (up to 6.5 MW/m^3). This radiation is mainly located in the inner divertor, whereas in the outer divertor there is almost no additional radiation compared to the phase between ELMs. The averaged radiated power is 5.7 MW, which corresponds to 31% of the sum of input and ELM power.

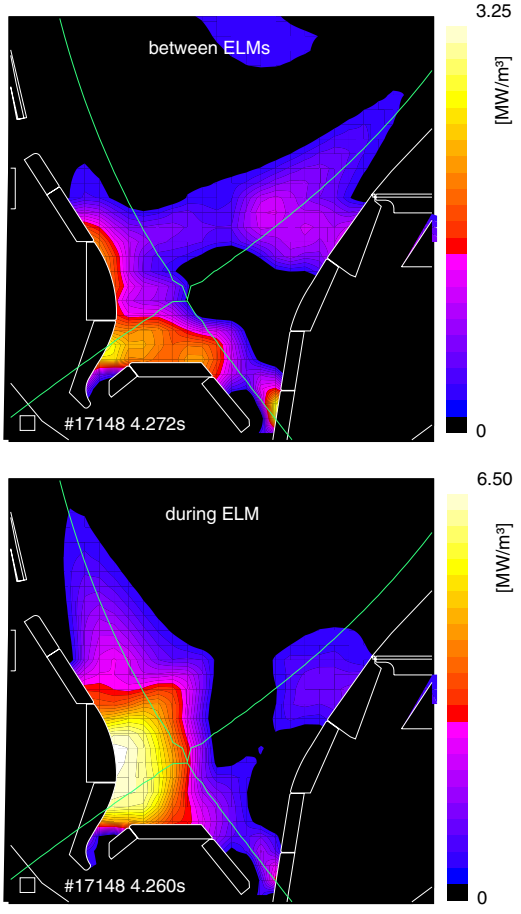

Fig. 2. Distribution of the averaged radiated power density in the divertor of ASDEX Upgrade during a 2 ms time interval between ELMs (top) and during an ELM (bottom). Note that the colour scale in the bottom picture is extended by a factor of two. The correct distribution is expected to be locally more concentrated, since the tomographic algorithm tends to smoothen it.

4. Dependence of the ELM radiation on plasma parameters

In order to investigate properties of ELMs, a series of discharges was performed in ASDEX Upgrade with scans of several plasma parameters, while trying to get comparable ELMs. These shots have also been used to investigate the ELM radiation.

Fig. 3 shows the dependence of the radiated energy due to an ELM on the normalised ELM energy E_{ELM}/W_{MHD}. The 'background radiation' between ELMs has already been subtracted, so that the values in Fig. 3 correspond to the additional radiation during an ELM.

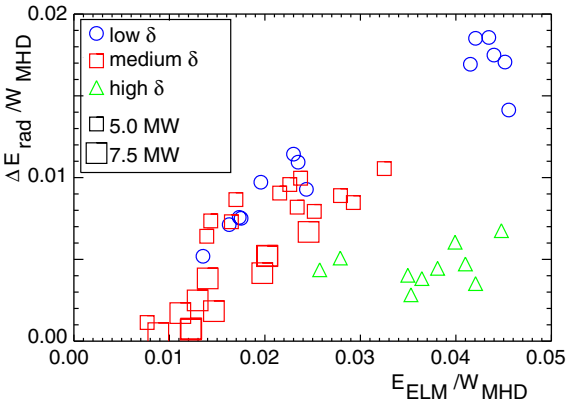

Fig. 3. Dependence of the radiated energy due to an ELM (scaled by the plasma energy) on the normalised ELM energy for different triangularities δ and heating powers.

The radiated energy due to an ELM increases for larger ELMs (with increasing normalised ELM energy), and correspondingly decreases with increasing ELM frequency. This behaviour is similar for discharges with both low ($\delta < 0.2$) and medium triangularities and medium (5 MW) and higher (>5 MW) heating power. For discharges with high triangularity ($\delta > 0.3$) however, the radiation during an ELM is clearly less than in otherwise similar discharges with medium or low triangularity. The reason for this dependence of the radiation on the plasma shape still has to be investigated. An artefact effect of the diagnostic or data evaluation can be eliminated, since the coverage of the plasma with bolometer lines of sight is good for all investigated plasma shapes.

Fig. 4 shows the dependence of the fraction of the radiated energy due to an ELM to the total ELM energy loss on the normalised ELM energy and on the electron density. Between 10% and 40% of the ELM energy are found as radiation, with a slight decrease for increasing normalised ELM energy or decreasing normalised density. Again, for discharges with higher triangularities the fraction of the ELM energy, which is found as radiation is less than for discharges with low or medium triangularity. Also for discharges with high heating power or high $q_{95} > 6$ the normalised ELM radiation is clearly less than for the discharges shown in Fig. 4.

The in–out-asymmetry of the ELM radiation, which was already mentioned in Fig. 2, is nearly independent of the plasma parameters. Whereas between ELMs the radiation is nearly symmetrical distributed between the inner and outer divertor (with an in/out ratio of the radiated energy of 60%/40%), the ELM itself radiates mainly only in the inner divertor (with an in/out ratio of 85%/15%) for nearly all investigated discharges. This in–out-asymmetry is also found in the measured heat fluxes to the divertor targets [5]. Only for high-q discharges the ELM radiation is more symmetrical distributed between the inner and outer divertor.

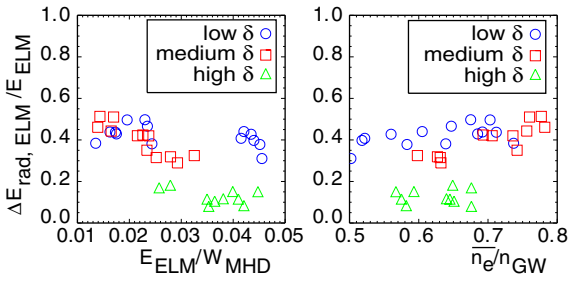

Fig. 4. Dependence of the normalised ELM radiation on the normalised ELM energy (left) and the normalised density (right) for discharges with 5 MW heating power and $q_{95} \approx 4.9$.

5. Energy balance

The energy balance is obtained by comparing the sum of the radiated energy and the power load to target plates (measured by thermographic cameras) with the sum of the heating energy and the loss of internal plasma energy. Here it was taken into account that a part $E_{\text{correction}}$ (up to 20% of the target load) of the divertor radiation is recorded by both the bolometers and the thermographic cameras [6]. Fig. 5 shows the time traces of these values for a time period of the discharge from Fig. 2, both between ELMs and during ELMs. In this discharge, the obtained energy balance is well fulfilled in both cases, as it is the case for most discharges with medium heating power (Fig. 6). For shots with higher heating power however, some parts (up to 50%) of the input energy are not found as radiation or power load. This missing energy may be deposited as power load on divertor targets or other in-vessel components not monitored by thermographic cameras [1], or on the first wall. No clear dependance on the triangularity could be found.

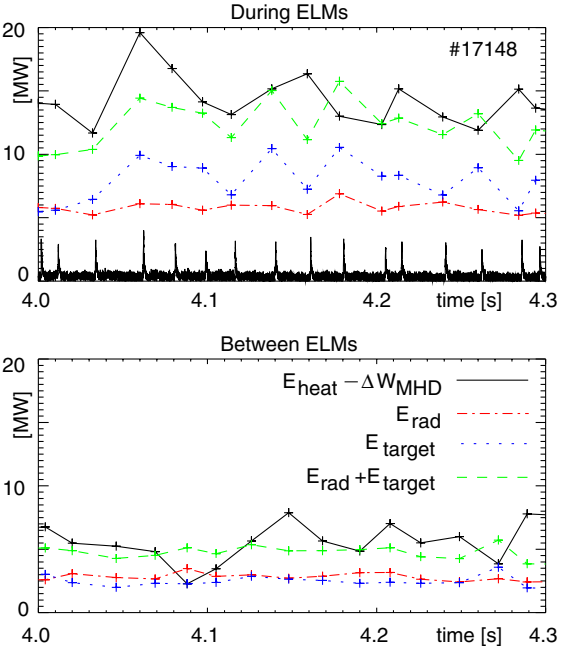

Fig. 5. Energy balance between ELMs (bottom) and during ELMs (top), showing the averaged radiated power (dash-dotted), the power load to the divertor target plates (dotted), the sum of these two values corrected by the part, which is recorded by both bolometers and thermographic cameras (dashed). This sum should be compared to the sum of input energy and loss of plasma energy (solid). In the upper picture the H_α radiation from the inner divertor is also indicated in arbitrary units.

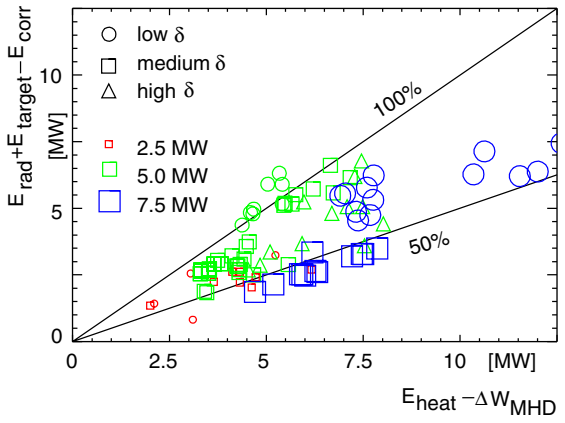

Fig. 6. Energy balance during ELMs comparing the averaged input power (heating plus ELM power) with the averaged power losses by radiation and heat load to target plates.

6. Conclusions

In ASDEX Upgrade about 50% of the ELM energy losses were found as target load in the divertor, and some 10–20% estimated on plasma facing components outside the divertor [1]. In order to explain the missing parts of the energy, the radiation during type-I ELMs has been investigated. It was found that the radiation due to the ELM (in addition to the 'background' radiation between ELMs) is mainly located in the inner divertor. Between 10% and 40% of the ELM energy is found as radiation. This normalised ELM radiation decreases slightly with increasing normalised ELM energy or decreasing electron density. It decreases clearly for discharges with higher heating power or higher q_{95}. The energy balance comparing heating energy plus ELM energy with energy losses by radiation and heat load to the target plates is nearly fulfilled during discharges with medium heating power. For shots with higher heating power some parts of the ELM energy (up to 50%) are not found and may be deposited as power load outside the divertor.

References

[1] A. Herrmann, T. Eich, V. Rohde, J.C. Fuchs, J. Neuhauser, et al., Plasma Phys. Control. Fus. 46 (6) (2004) 971.
[2] K.F. Mast, J.C. Vallet, C. Andelfinger, et al., Rev. Sci. Instrum. 63 (3) (1991) 744ff.
[3] J.C. Fuchs, K.F. Mast, D. Coster, A. Herrmann, R. Schneider, et al., Contribution 26th EPS (1999) 1385.
[4] J.C. Fuchs, K.F. Mast, A. Herrmann, K. Lackner, et al., Contribution 21st EPS (1994) 1308ff.
[5] A. Herrmann, T. Eich, S. Jachmich, M. Laux, P. Andrew, et al., J. Nucl. Mater. 313–316 (2003) 759.
[6] J.C. Fuchs, D. Coster, A. Herrmann, A. Kallenbach, K.F. Mast, et al., J. Nucl. Mater. 290–293 (2001) 525.